Effectiveness Analysis of Physical Carrier-sensing in IEEE 802.11 Wireless Networks

Fu-Yi Hung
Department of Innovative Information and Technology
Tamkang University

Abstract: Physical carrier-sensing mechanism has been used as an effective way to alleviate interference in wireless networks, but it also constrains spatial reuse. The aggregate throughput in wireless ad hoc networks is a tradeoff between spatial reuse and interference avoidance. The influence of physical carrier-sensing on the aggregate network throughput has attracted several studies. Previous work investigated the interference with the packet reception at receivers and proposed the optimal carrier-sensing range to achieve the maximum aggregate throughput. However, the interference with the sender's reception of the receiver's acknowledgement (ACK) has been ignored. In this paper, we consider the influence of interference at both senders and receivers on the aggregate throughput in wireless ad hoc networks. We propose a spatiotemporal model that describes the effectiveness of the physical carrier-sensing mechanism.

Keywords: physical carrier-sensing mechanism, wireless ad hoc network, IEEE 802.11

摘要: 實體層載波偵測機制能夠有效的減輕無線網路中的干擾，但是這機制也限制了空間的再利用。在一個無線隨意網路中，總傳輸量是空間再利用與干擾抑制兩個因素之間的妥協。實體層載波偵測對於無線網路總傳輸量的影響吸引了不少的研究。先前的工作，研究了干擾對於接收器接收封包的影響，並提出最佳的載波偵測範圍，以獲得最大的總傳輸量。但是，這些研究忽略了，當傳送器接收確認訊息(ACK)時，也會受到干擾的影響。在本文中，我們同時考慮了干擾對於傳送器與接收器的影響，並運用一個時間暨空間模型，來分析實體層載波偵測機制的有效性。

關鍵字: 實體層載波偵測機制、無線隨意網路、IEEE 802.1

Introduction: IEEE 802.11 standard [1] is widely used in wireless ad hoc networks because its distributed coordination function (DCF) can support self-organizing peer-to-peer communication without the need for configuring the infrastructure network. The DCF is a random channel-access scheme where each station can initiate its transmission based on its sensing of the channel state. This scheme unavoidably introduces packet collisions because of multiple simultaneous transmissions on the same channel without a centralized coordination. To mitigate the packet collisions, the DCF uses Carrier Sense Multiple Access with Collision Avoidance (CSMA/CA) and an exponential backoff procedure. CSMA/CA defines two channel states, *idle* and *busy*, through the physical and virtual carrier-sensing mechanisms. In DCF, a station has to sense the channel state before transmitting a packet. If the channel is sensed as idle then the station transmits the packet; otherwise, it defers its transmission for a random period of time by executing the backoff procedure and then sensing the channel again. In physical carrier-sensing mechanism, if a station can detect the transmitted signal on the channel (if the energy level of the signal exceeds a predefined threshold), then its Clear Channel Assessment (CCA) mechanism shall report the channel as busy; otherwise it considers the channel as idle. This threshold is called physical carrier-sensing (PCS) threshold. Another method called virtual carrier-sensing mechanism is an optional mechanism in CSMA/CA. It uses the Request-to-Send (RTS) / Clear-to-Send (CTS) dialogue to let the other stations know the length of time to defer their transmissions and avoid packet collisions. However, the RTS/CTS access method is designed mainly to support wireless local area networks (LANs) and is not effective in wireless ad hoc networks [2-3].

In a wireless network, the channel state sensed by the sender is not always the same as that sensed by the receiver, which results in the exposed and hidden station effects [4]. The *hidden stations* are those which should suspend their transmission but fail to do so because they cannot hear the sender's transmission. Their transmission can corrupt the sender's packet reception at the receiver. This problem is due to the fact that the PCS threshold is set too high so the sender and hidden stations fail to detect each other's transmission. If the PCS threshold can be adjusted, decreasing this threshold can alleviate the interference from hidden stations, which will lead to increased aggregate throughput. However, decreasing the PCS threshold will decrease the spatial reuse and might increase the number of exposed stations, which will decrease the aggregate throughput. The *exposed stations* defer their transmission when they sense sender's transmission, although their transmission would not interfere with the reception of the sender's packet. As the PCS threshold decreases, the aggregate throughput does not decrease or increase monotonically because the throughput is a tradeoff between the interference and spatial reuse.

The topic of setting the optimal carrier-sensing range has attracted several studies. Ye et al. [5] proposed a spatial reuse index that represents the effectiveness of the virtual carrier-sensing based on the sender-receiver distance. They found that the virtual carrier-sensing threshold is optimal when the transmission range equals the interference range. However, the physical carrier-sensing is ignored in their study. According the path-loss model, Zhu et al. [6] derived the optimal PCS threshold that maximizes the aggregate throughput in mesh networks. Their study showed that a network achieves its maximum throughput when the physical carrier-sensing range equals the interference range. This optimal range is based on two assumptions: (a) the interference range is much larger than the transmission range; and (b) background noise is negligible. However, based on the path-loss model and SINR (signal-to-interference-noise ratio), the assumption (a) is valid only when the sender-receiver distance is close to the transmission range. Also, these two assumptions are mutually inconsistent. When the sender-receiver distance is close to the

transmission range, background noise results in the interference range becoming much larger than the transmission range. Yang et al. [7] showed that the MAC layer overhead has a large impact on the choice of the PCS threshold. The MAC layer overhead is mainly determined by the data rate and packet size. However, their simulation results showed that the optimal PCS threshold only slightly changes with the packet size. Their results also showed that the optimal PCS threshold is lower than the SINR value by about 2 to 4 dB. Their results also imply that the optimal physical carrier-sensing range is larger than the interference range by about 19% to 41% for the data rates of 18, 36 and 54 Mbps. On the other hand, Zhai et al. [8] proposed that different data rates have a similar optimal PCS threshold. They validated their approach by ns-2 simulation in one-hop and multi-hop wireless ad hoc networks. However, their optimal PCS threshold is not practical in real networks, because they set the physical carrier-sensing range lower than the transmission range of most data rates. In real wireless networks, for a given data rate, the physical carrier-sensing range is equal to or greater than the transmission range. Lin & Hou [9] proposed a model that balances the interplay of spatial reuse and spectrum efficiency. Their analytical model showed that there are two or more optimal physical carrier-sensing ranges where the network throughput reaches its peak value. Ma et al. [10], who developed an analytical model that determines the optimal PCS threshold for a homogenous wireless network with constant link distances. Their results showed that a close-to-optimal value of the carrier-sensing range is equal to the interference range. However, their model results are not consistent with their simulation results which showed that the optimal carrier-sensing range is larger than the interference range by about 20%.

The rest of this paper is organized as follows. In section II, we present the propagation- and interference analytical models. In section III, we evaluate the effectiveness of the physical and virtual carrier-sensing mechanisms through spatial and temporal analysis. In section IV, we compare our analytical results with those obtained by ns-2 simulations. Finally, we discuss conclusions in section V.

II. Interference Model

The radio propagation model used in this paper is the path-loss model given by

$$P_r = \frac{P_t}{d_t^n} \qquad (1)$$

where P_r is the received signal strength at the receiver, P_t is the transmission power at the sender, d_t is the distance between the sender and the receiver, and n is the path-loss exponent depending on the propagation environment [11]. We assume all stations in our network use the same transmission power P_t. Based on this model and 802.11 protocol, we can define three ranges: transmission range (R_t), carrier-sensing range (R_c) and interference range (R_i) as follows.

(a) **Transmission range** (R_t) is the maximum distance between a sender and a receiver at which the receiver can correctly decode frames from the sender in the presence of noise but no interference. The correct decoding in case of IEEE 802.11b direct-sequence spread-spectrum (DSSS) means the frame error rate (FER) must be lower than 8×10^{-2} for MAC-layer packets of 1024 bytes if the signal-to-noise ratio (SNR) at the receiver is higher than a threshold $S_0 = -80$ dBm [1]. It is given by

$$SNR(d_t = R_t) = S_0 = \frac{P_r(d_t = R_t)}{N} = \frac{P_t / R_t^n}{N} \qquad (2)$$

where N is the noise power.

(b) **Physical carrier-sensing range** (R_c) is the maximum distance between a sender and a receiver at which the receiver can sense the signal transmitted from the sender but may not be able to correctly decode frames. Based on the clear-channel-assessment (CCA) of the 802.11 protocol, a station shall report the channel state as busy if it senses the energy greater than the energy detection (ED) threshold (≤ -80 dBm for 802.11b DSSS [1]).

(c) **Interference range** (R_i) is the maximum distance between a second sender (interfering source) and a receiver at which the signal transmitted from the second sender can interfere with the frame reception at the receiver and cause the FER to be higher than the requirement. At this distance, the SINR is equal to S_0 and given by

$$SINR(d_i = R_i) = S_0 = \frac{P_r}{P_i(d_i = R_i) + N} = \frac{(P_t / d_t^n)}{(P_t / R_i^n) + N} \qquad (3)$$

where P_i is the received interference strength at the receiver, and d_i is the distance between the second sender and the receiver. Based on eq. (3), the interference range can be represented as [10]:

$$R_i = R_t \cdot \left(\frac{S_0}{(R_t / d_t)^n - 1} \right)^{\frac{1}{n}} \qquad (4)$$

This range is not fixed and depends on the sender-receiver distance. Based on this interference model, we present an effectiveness analysis of the physical carrier-sensing mechanism in wireless ad hoc networks as follows.

III. Effectiveness Analysis of the Physical Carrier-sensing Mechanism

A. Spatiotemporal Analysis of the Physical Carrier-sensing: We classify all scenarios into three spatial configurations based on the size of the interference range because the interference range is a function of the sender-receiver distance. The following assumptions are used in our analysis: (i) the channel between any two stations in the network is identical in terms of path loss; (ii) the transmit power of all stations is identical; (iii) the transmission range, carrier-sensing range, and interference range are all circular in shape; (iv) the physical carrier-sensing range is set equal to the transmission range in this section of the paper (for spatiotemporal analysis).

We define the following three station types based on the coverage of the interference and physical carrier-sensing ranges.

(a) The *covered stations* are the stations for which their transmission can interfere with the packet reception at the receiver or sender. They can sense and decode the transmission between the sender and receiver to suspend their transmission.

(b) The *hidden stations* are the stations for which their transmission can interfere with the packet reception at the receiver or acknowledgement reception at the sender. They cannot sense or decode the transmission between the sender and receiver.

(c) The *exposed stations* are the stations for which their transmission cannot interfere with the packet reception at the receiver or ACK reception at the sender. They can sense or

decode the transmission between the sender and receiver to suspend their transmission.

Configuration-1: $R_i < (R_t - d_t)$

When the sender-receiver distance plus the interference range is smaller than the transmission range (Fig. 1a), the whole interference range of receiver B is within the transmission range of sender A, the sender-receiver distance is given by

$$0 \leq d_t < (R_t - R_i) \tag{8}$$

For example, setting the SINR as 6.02 dB and path-loss exponent as 4, the interval of the sender-receiver distance in Configuration-1 is

$$0 \leq d_t < 0.38R_t \tag{9}$$

In this configuration, there are no hidden stations because all potential interfering stations are covered, inside zone 1 in Fig. 1a. When sender A transmits a packet to receiver B (Fig. 1b), these covered stations can decode this data frame from sender A and ACK frame from receiver B, so they will suspend their transmission until they sense the channel as idle again. The possible collision period between two stations is called the *vulnerable period*. This period for a covered station relative to the sender is the minimum period of time from the time that the sender starts to transmit a data frame to the time that the covered station detects this ongoing transmission. In IEEE 802.11, this period of time is defined as one *backoff slot time*, shown in Fig. 1b. So, the physical carrier-sensing mechanism is effective in reducing interference in this configuration. On the other hand, the stations inside the transmission ranges of the sender or receiver but outside the interference ranges of both the sender and receiver are exposed stations as shown inside white zone in Fig. 1a. They are not potential interfering stations relative to the sender or receiver but are suspended to transmit packet simultaneously.

Configuration-2: $(R_t - d_t) \leq R_i < R_t$

When the interference range is larger than that in Configuration-1 but smaller than the transmission range (Fig. 2a), the sender-receiver distance is

$$(R_t - R_i) \leq d_t < (R_t / \sqrt[n]{S_0 + 1}) \tag{10}$$

If the SINR is set at 6.02 dB and path-loss exponent as 4, the interval of the sender-receiver distance in Configuration-2 is

$$0.38R_t \leq d_t < 0.61R_t \tag{11}$$

The sender A's transmission range covers most part of the interference range as zones 1 and 2 in Fig. 2a. The zones 1 and 2 are called the *covered stations area*. On the other hand, the stations inside the zone 3 in Fig. 2a are the hidden stations relative to sender A. They are inside the interference range of receiver B but outside the transmission range of sender A. The zone 3 is called the *hidden stations area*. This zone becomes larger as the transmitter-receiver distance grows. When sender A transmits a data frame to receiver B (Fig. 2b), these hidden stations in zone 3 cannot sense the data frame transmitted by sender A. Before sensing the ACK frame transmitted from receiver B, they could transmit their packets simultaneously and this might interfere with the reception of A's data frame at the receiver B. The vulnerable period with respect to the hidden stations in zone 3 is the length of a data frame (Fig. 2b).

Configuration-3: $R_i > R_t$

When the interference range is larger than the transmission range (Fig. 3a), the sender-receiver distance is given by

$$(R_t / \sqrt[n]{S_0 + 1}) \leq d_t \leq R_t \tag{12}$$

If the SINR is set at 6.02 dB and path-loss exponent as 4, the interval of the sender-receiver distance in Configuration-3 is

$$0.61R_t \leq d_t < R_t \tag{13}$$

The sender A's transmission range covers a small part of the interference range as zones 1 and 2 in Fig. 3a. The zones 1 and 2 are called the *covered stations area*. The stations inside zone 3, 4 and 5 in Fig. 3a are hidden stations to the sender and their transmission can interfere with data frame reception at the receiver. The vulnerable period with respect to the hidden stations in these zones is the length of a data frame (Fig. 3b). In addition to these stations that are hidden to the sender, the stations inside zones 5 and 6 in Fig. 3a are semi-hidden stations (hidden to the receiver), because they can interfere with ACK reception on the sender. The vulnerable period with respect to the hidden stations in zones 5 and 6 is the length of an ACK frame (Fig. 3b). Both the receiver and sender suffer from the hidden station problem in

this configuration. The zones 3, 4, 5 and 6 are called the *hidden stations area*. The physical carrier-sensing mechanism is effective only in preventing interference from the covered stations area, but is not effective in alleviating interference from the hidden stations area. However, in reality the size of hidden stations area is much larger than that of the covered stations area. The effectiveness of the physical carrier-sensing mechanism is low in Configuration-3. Unfortunately, this configuration is the most common situation in real-world wireless ad hoc networks. We will prove this claim in section III.B.
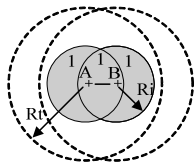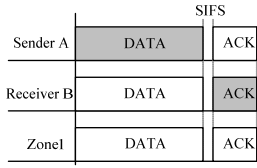
a. Spatial analysis   b. Temporal analysis
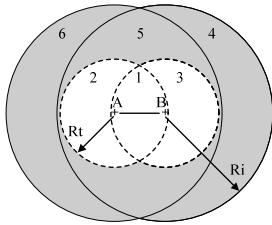Fig. 1 Spatial and temporal analysis of the physical carrier-sensing mechanism in Configuration-1
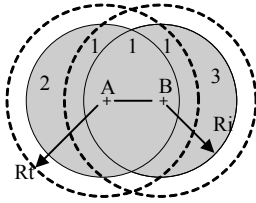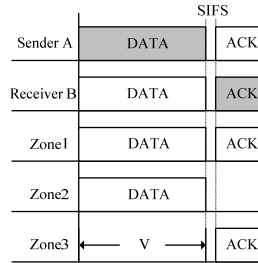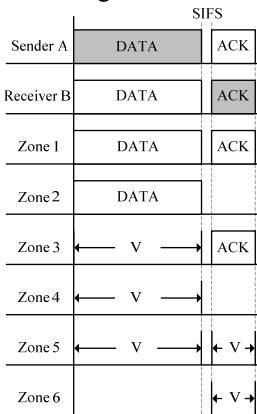

V = Vulnerable period
a. Spatial analysis   b. Temporal analysis
Fig. 2 Spatial and temporal analysis of the physical carrier-sensing mechanism in Configuration-2

V = Vulnerable period
a. Spatial analysis   b. Temporal analysis
Fig. 3 Spatial and temporal analysis of the physical carrier-sensing mechanism in Configuration-3

B. Influence of the System Parameters on the Effectiveness of the Physical Carrier-sensing: The spatiotemporal analysis shows that the larger the interference range, the lower the effectiveness of the physical carrier-sensing mechanism, particularly in Configuration-3. The interference range depends not only on the sender-receiver distance as discussed in section III.A, but also other parameters such as SINR threshold, path-loss exponent and the number of interfering stations. The influence of these parameters on the effectiveness of the physical carrier-sensing mechanism is discussed next.

First, we present the interference range in case of a single data rate, a fixed path-loss exponent and a single interfering station. We set the data rate at 6 Mbps, the SINR threshold at 6 dB, the path-loss exponent at 4, and the transmission range at 1 meter. Based on the interference model, equation (4), the interference range increases almost linearly when the sender-receiver distance is less than 0.61 meter; after the sender-receiver distance exceeds 0.61 meter, the interference range grows quickly and nonlinearly, and its value approaches the infinity when the sender-receiver distance equals to the transmission range (Fig. 4). In addition, as the sender-receiver distance exceeds 0.61 meter, the interference range exceeds the transmission range (1 meter). This scenario represents the Configuration-3.

(i) Multi-rate Mechanism
IEEE 802.11 standard defines multiple data rates to support reliable transmission on channels of different quality. In general, a higher data rate requires higher receiver sensitivity and higher SINR to achieve the same bit-error-rate (BER) as a lower data rate. Higher receiver sensitivity results in the shorter the transmission range (Table I). The transmission ranges in Table I are calculated based on the propagation model in equation (1) and the following assumption: path-loss exponent equals 4, the transmission range of the 6 Mbps rate is 1 meter, and all stations are using a fixed transmit power for all data rates. On the other hand, based on the interference model in equation (4), a higher data rate with a higher SINR threshold causes a larger interference range, given a fixed sender-receiver distance (Fig. 5).

In order to maximize the throughput, the multi-rate mechanism will use the highest rate among the available rates, based on the channel quality between the sender and receiver. For example, according to the receiver sensitivity in Table I, if the received signal is −80dBm, then the 9 Mbps and 6 Mbps rates are available. The highest available rate (in this case, 9 Mbps) will be selected as the transmission rate. According to this mechanism, the 9 Mbps rate will be used only when the received signal power is between the receiver's sensitivity for 9 Mbps (i.e., −81 dBm) and that for 12 Mbps (i.e., −79 dBm). This means that each rate will be used near its transmission limit, except for the highest rate. In addition, the actual interference range under the multi-rate mechanism is the zigzag envelope in Fig. 5, because a station always uses the highest rate among the currently available rates.

We assume that the lowest data rate, 6 Mbps, is used to transmit the physical layer header of all packets, and we set its transmission range at 1 meter. When a sender transmits a data frame to a receiver at a higher data rate of 54 Mbps, it transmits the physical header at 6Mbps rate and the data payload at 54 Mbps rate. The stations inside the 1 meter range from the sender can sense this data frame but may not be able to decode this data payload if they are outside the transmission range of the 54 Mbps rate. When the sender-receiver distance exceeds 0.35 meters (Fig. 5), the interference range exceeds 1 meter. This is the scenario of Configuration-3. Compared to the interference range of a single data rate of 6 Mbps in Fig. 4, the multi-rate mechanism significantly increases the probability that Configuration-3 will occur and reduces the effectiveness of the physical carrier-sensing mechanism.

(ii) Path-loss Exponent
The path-loss exponent represents the rate of the average received-signal-power decline as the sender-receiver distance increases. Its value depends on the propagation environment. If the transmit power is set at −42 dBm in the propagation model of equation (1), the transmission ranges of 6 Mbps rate are 100 meters, 21.5 meters, 10 meters, and 6.3 meters when the path loss exponent is set at 2, 3, 4, and 5, respectively. The transmission range decreases

when the path-loss exponent increases. To compare the influence of the path-loss exponent on the interference range, the transmission ranges of all path-loss exponents are normalized as 1. As the sender-receiver distance increases, the interference range in low path-loss exponent environment increases faster than that in high path-loss exponent environment (Fig. 6). When the path-loss exponent is 2 and the sender-receiver distance exceeds 38% of the transmission range, the corresponding interference range exceeds the transmission range. However, when the path loss exponent is 5 and the sender-receiver distance exceeds 68% of the transmission range, the corresponding interference range exceeds the transmission range (Fig. 6). This result indicates that, the lower the path-loss exponent, the lower the effectiveness of the physical carrier-sensing mechanism.

(iii) Number of Interfering Stations
If two or more interfering stations transmit simultaneously with the sender, the packet reception at the receiver is interfered by the accumulated interfering signal. There are many parameters that can affect the accumulated interfering signal strength, such as the number of the interfering stations, the receiver-to-interfering-station distance, and the transmit power. It is very hard to define the interference range in a multiple interfering station scenario, even in a simple two-interfering-station case. Suppose that in a wireless network the sender-receiver distance is fixed. Two interfering stations use a fixed transmit power (P_t) and they transmit simultaneously with the sender. The accumulated interfering signal strength (P_{i_sum}) at the receiver is given by

$$P_{i\_sum} = P_i(1) + P_i(2) = \frac{P_t}{[d_i(1)]^n} + \frac{P_t}{[d_i(2)]^n} \quad (14)$$

where $P_i(1)$ and $P_i(2)$ are the signal strengths from the interfering stations 1 and 2 at the receiver, the $d_i(1)$ and $d_i(2)$ are the distances between the receiver and interfering stations 1 and 2. If the transmit power, path-loss exponent and the accumulated interfering signal strength at the receiver are known, equation (14) still has two unknown parameters, $d_i(1)$ and $d_i(2)$. There is infinite number of solutions for $d_i(1)$ and $d_i(2)$. So, it is very hard to define an appropriate interference range that represents the interfering

station topology in multiple interfering stations scenarios.

To simplify the interference range definition in multiple interfering stations scenarios, we assume that the simultaneous interfering stations have the same receiver-interfering-station distance and the same transmit power. Of course, this scenario is very rare in real wireless networks. Based on these assumptions, the SINR can be represented as

$$SINR(d_i = R_i) = S_0 = \frac{(P_t / d_t^n)}{m \cdot (P_t / R_i^n) + N} \qquad (15)$$

where ΣP_i is the accumulated interference strength at the receiver, m is the number of the interfering stations, and R_i is the interference range in the multiple interfering stations scenario. Based on equation (13), the interference range is given by

$$R_i = R_t \cdot \left(\frac{m \cdot S_0}{(R_t / d_t)^n - 1} \right)^{\frac{1}{n}} \qquad (16)$$

When the sender-receiver distance increases, the interference range grows more quickly in the case of a large number of the interfering stations than that with a few interfering stations, assuming that all interfering stations use the same transmit power (Fig. 7). This result indicates that, the greater the number of the interfering stations, the lower the effectiveness of the physical carrier-sensing mechanism.
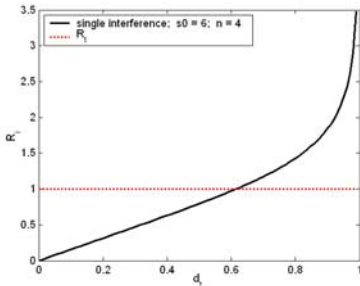

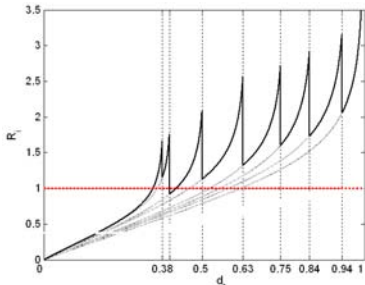Fig. 4 The interference range as a function of the sender-receiver distance.

Fig. 5 The influence of the 802.11g multi-rate
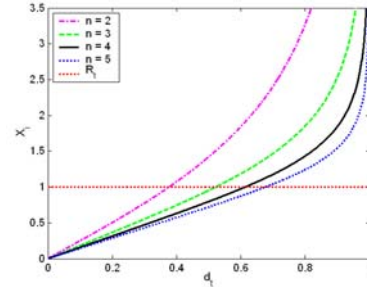
mechanism on the interference range.

Fig. 6 The influence of the path-loss exponent on the interference range.
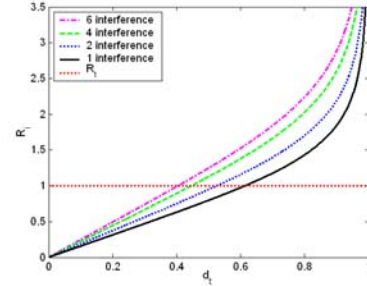

Fig. 7 The influence of the number of the interfering stations on the interference range.

TABLE I
SINR AND RECEIVER SENSITIVITY
FOR STANDARD DATA RATES OF IEEE 802.11g [12]

Rates (Mbps)	Receiver sensitivity (dBm)	SINR (dB)	Transmission range R_t (m)
54	−65	24.56	0.38
48	−66	24.05	0.40
36	−70	18.80	0.50
24	−74	17.04	0.63
18	−77	10.79	0.75
12	−79	9.03	0.84
9	−81	7.78	0.94
6	−82	6.02	1.00

We calculated R_t based on eq. (1)

VI. Performance Evaluation
In this section, we evaluate the spatial-analytical described above, to determine the optimal physical carrier-sensing range of ad hoc wireless networks, and compare with the results obtained by ns-2 simulator.

The Configuration-3 is the most frequent scenario in real wireless ad hoc networks where the interference range is larger than the transmission range, as shown in section III.A. The distance between two adjacent stations is set at 95m so the

interference range is about 227m, according to equation (4). The interference range is more than double the transmission range. As the physical carrier-sensing range increases from the lower bound up to 276m, the aggregate throughput also increases quickly and reaches its maximum at about 17 Mbps (Fig.8). Then it decreases gradually as the physical carrier-sensing range exceeds 276m. The optimal physical carrier-sensing range in this scenario equals 276m. The throughput obtained by our performance model is consistent with that obtained by ns-2 simulation. On the other hand, the function f reaches the minimum when the physical carrier-sensing range equals the interference range, at 227m. If the physical carrier-sensing range is set according to the spatial-analytical model, the achieved throughput will be by about 22% lower than the throughput achieved by using the optimal physical carrier-sensing range given by our Markov-chain model. This is because the areas of the zones with hidden and exposed stations do not accurately represent the numbers of the stations in these zones.
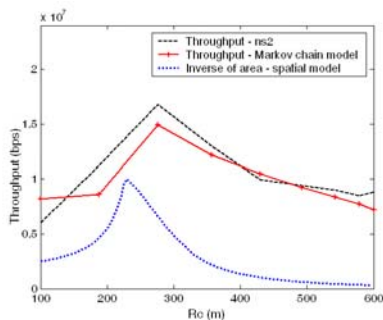

Fig. 8 Throughput for Configuration-3

V. Conclusion: We present a spatiotemporal model that characterizes the effectiveness of the physical carrier-sensing mechanism in wireless ad hoc networks. In addition to the interference with packet reception at receivers, as modeled in previous work, our model includes semi-hidden stations that interfere with the reception of acknowledgements at senders. This model shows that the physical carrier-sensing mechanism is not effective in Configuration-3, which it is the most frequently occurring scenario in real wireless ad hoc networks.

References

[1] ANSI/IEEE Std 802.11: Wireless LAN Medium Access Control (MAC) and Physical Layer (PHY) Specification, 1999.

[2] S. Xu, and T. Saadawi, "Does the IEEE 802.11 MAC protocol work well in multihop wireless ad hoc networks?" IEEE Commun. Magazine, vol. 39, no. 6, pp. 130-13, June 2001.

[3] K. Xu, M. Gerla, and S. Bae, "How effective is the IEEE 802.11 RTS/CTS handshake in ad hoc networks?" Proc. of IEEE Globecom, pp. 72-76, November 2002.

[4] F. A. Tobagi and L. Kleinrock, "Packet switching in radio channels: Part II," IEEE Trans. Commun., vol. 23, no. 12, pp. 1417-1433, December 1975.

[5] F. Ye, S. Yi and B. Sikdar, "Improving spatial reuse of IEEE 802.11 based ad hoc networks," Proc. of IEEE Globecom, pp. 1013-1017, December 2003.

[6] J. Zhu, X. Guo, L. L. Yang, W. S. Conner, S. Roy, and M. M. Hazra, "Adapting physical carrier-sensing to maximize spatial reuse in 802.11 mesh networks," Wiley J. Wireless Commun. Mob. Comput., vol. 4, no. 8, pp. 933-946, December 2004.

[7] X. Yang and N. H. Vaidya, "On the physical carrier sense in wireless ad hoc networks," Proc. of IEEE INFOCOM, pp. 2525-2535, March 2005.

[8] H. Zhai and Y. Fang, "Physical carrier sensing and spatial reuse in multirate and multihop wireless ad ho networks," Proc. of IEEE INFOCOM, April 2006.

[9] T.Y. Lin and J. C. Hou, "Interplay of spatial reuse and SINR determined data rates in CSMA/CA-based, multi-hop, multi-rate wireless networks," Proc. of IEEE INFOCOM, pp. 803-811, May 2007.

[10] H. Ma, R. Vijaykumar, S. Roy and J. Zhu, "Optimizing 802.11 mesh networks performance using physical carrier-sensing," accepted for publication in *IEEE/ACM Trans. on Networking*.

[11] T. S. Rappaport, Wireless Communications: Principles and Practices, 2nd Ed., Prentice Hall, 2002.

[12] J. Yee and H. Pezeshki-Esfahani, "Understanding wireless LAN performance trade-offs," CommsDesign.com, November 2002.